STD: Student's t-Distribution of Slopes for Microfacet Based BSDFs

Mickaël Ribardière, Benjamin Bringier, Daniel Meneveaux, Lionel Simonot

STD: Student's t-Distribution of Slopes for Microfacet Based BSDFs

Mickaël Ribardière, Benjamin Bringier, Daniel Meneveaux, Lionel Simonot

STD: Student's t-Distribution of Slopes for Microfacet Based BSDFs

M. Ribardière[1], B. Bringier[1], D. Meneveaux[1], L. Simonot[2]

[1] University of Poitiers - XLIM Institute - UMR CNRS 7252
[2] University of Poitiers - Pprime Institute - UPR CNRS 3346

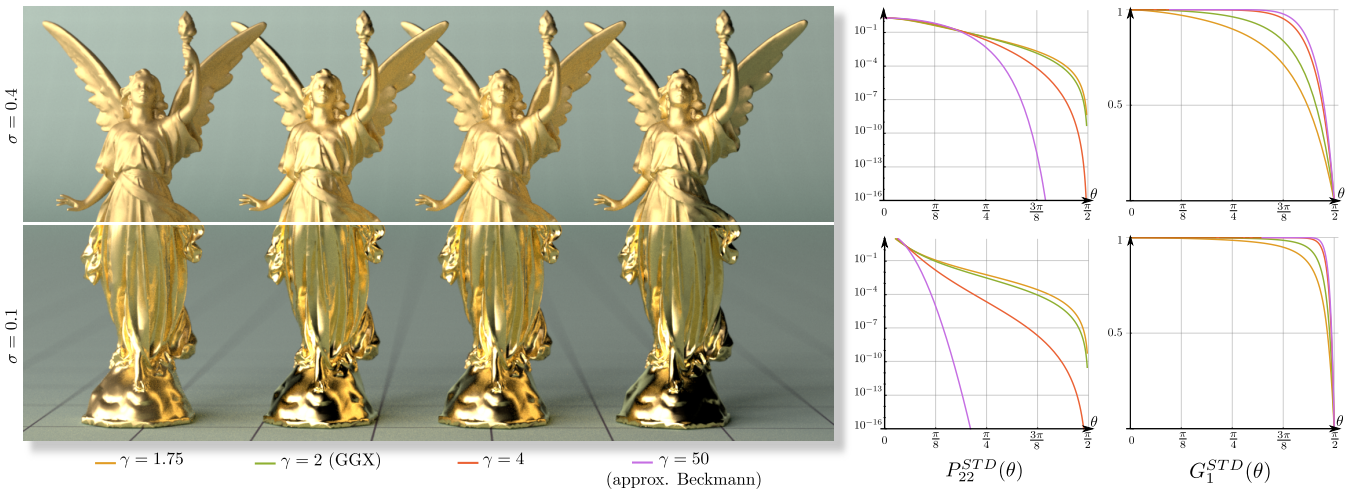

Figure 1: *Appearance variations of a gold object, according to various roughness parameters of Student's t-Distribution (STD) of slopes. Thanks to a single additional parameter γ, STD generalizes the well-known Beckmann's (when $\gamma \to \infty$) and GGX (when $\gamma = 2$) distributions; it provides the Smith's analytical geometric attenuation factor (GAF) for an infinite set of distribution configurations, as well as importance sampling functions. The curves illustrate slope distributions P_{22}^{STD} (log scale) and the corresponding GAF functions G_1^{STD}.*

Abstract

This paper focuses on microfacet reflectance models, and more precisely on the definition of a new and more general distribution function, which includes both Beckmann's and GGX distributions widely used in the computer graphics community. Therefore, our model makes use of an additional parameter γ, which controls the distribution function slope and tail height. It actually corresponds to a bivariate Student's t-distribution in slopes space and it is presented with the associated analytical formulation of the geometric attenuation factor derived from Smith representation. We also provide the analytical derivations for importance sampling isotropic and anisotropic materials. As shown in the results, this new representation offers a finer control of a wide range of materials, while extending the capabilities of fitting parameters with captured data.

Categories and Subject Descriptors (according to ACM CCS):

1. Introduction

The representation of materials is a crucial issue for rendering realistic environments, and many authors have been interested in physically plausible models, not only for computer graphics but also for many other areas such as computer vision or augmented reality. Despite the numerous advances in the past thirty years, the definition of a generic mathematical description still remains a difficult challenge for several reasons: The model should be able to reproduce a wide range of visual appearances, it should be reciprocal and pre-

serve energy (physical plausibility), it should be straightforward to implement and efficient with lighting simulation systems.

Amongst the existing physically plausible models, distributions of microfacets have been favored by many authors for their ability to represent a wide range of surfaces [WMLT07, Hei14, JdJM14]. They are based on the product of three functions:

1. The BSDF f^{μ} associated with the microfacets, often considered as purely specular in most cases [CT82, BSH12], though some authors have also studied non-specular microfacets [ON94, WMLT07, DHI*13].
2. The distribution D of microfacet normals describes the surface roughness, controlling the specular lobe of which our visual attention is very sensitive. This function is crucial in the definition of a general BSDF representation, and many studies have focused on its representation [BS63, Sto67, TR75, CTL89, ON94, Sch94, WMLT07, BSH12, Bur12, LKYU12].
3. The geometric attenuation factor G (or GAF) accounts for masking and shadowing. It has also drawn much attention since the pioneering work proposed by Smith [Smi67] and Torrance and Sparrow [TS67]. Smith's approach is presently considered as physically more realistic, and the GAF function should be associated with the distribution function [Smi67, APS00, BBS02, WMLT07, Hei14]. This latter can be precomputed [APS00], but an analytical integration is preferable for a more general use. To our knowledge the analytical Smith's formulation of the GAF has been expressed for only two distributions: Beckmann's and GGX.

This paper proposes a normal distribution D^{STD}, which extends both Beckmann's and GGX distributions [BS63, TR75, WMLT07], thanks to a single additional parameter γ. It provides an additional control on the distribution slope and tail, providing an infinite set of configurations. Our function is inspired from the Generalized-Trowbridge-Reitz distribution [TR75, Bur12], with the advantage of making it possible to derive the associate analytic Smith-Bourlier shadowing and masking function as well as importance sampling. Such a practical generalization has never been proposed in computer graphics to our knowledge. More precisely, the main contributions of this paper are:

- the definition of a distribution function, corresponding to a bivariate Student's t-distribution in slopes space, which includes Beckmann and GGX for specific values of γ;
- the derivation of the corresponding analytic Smith-Bourlier geometric attenuation function;
- the mathematical derivation for importance sampling functions, and anisotropic representations;
- a representation dedicated to discrete values of γ, which is simpler and faster than the general model;
- an approximate function for the general case, which also accelerates the BRDF estimation, making the computation time equivalent to usual distribution functions (such as Beckmann's and GGX for instance).

The remainder of this paper is organized as follows: Section 2 sets the notations and the mathematical background; Section 3 provides our distribution function as well as the derived GAF and the importance sampling functions; Section 5 shows material and performance comparisons; Section 6 concludes and presents future work.

2. Background and problem statement

The BSDF $f(i,o,n)$ is defined as the ratio between: (i) The radiance reflected in an elementary solid angle $d\omega$ of direction o, by a surface element dS of normal n; (ii) The light flux coming from direction i in a solid angle $d\omega_i$ on dS (Figure 2):

$$f(i,o,n) = \frac{dL(o,n)}{dE(i,n)} = \frac{dL(o,n)}{L(i,n)\cos\theta_i d\omega_i}.$$

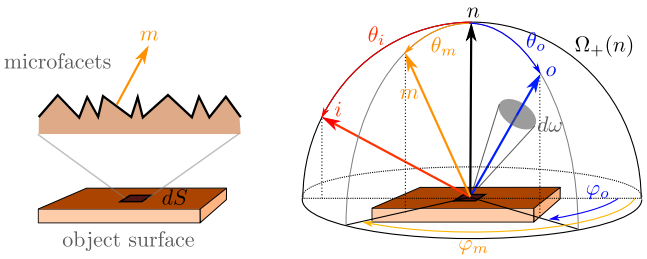

Figure 2: *Geometry of reflexion, based on a surface element dS of normal n, for an incident light flux coming from direction i and reflected towards direction o around a solid elementary angle dω. Microfacet orientation is defined by a normal m.*

Microfacet models consider the surface element dS as a statistical distribution of small facets, each of which is characterized by a normal direction m. All the microfacets share a common local BSDF $f^{\mu}(i,o,m)$. The global surface BSDF f thus corresponds to the integration of all the microfacet contributions from i to o. The general model is given by the following equation [TS67, ON94, WMLT07]:

$$f(i,o,n) = \int_{\Omega_+(n)} \frac{|im|}{|in|} f^{\mu}(i,o,m) \frac{|om|}{|on|} D(m) G(i,o,m)\, dm \qquad (1)$$

where $D(m)$ corresponds to the distribution of microfacet normals m, and $G(i,o,m)$ expresses the geometrical attenuation factor (or *GAF*); the notation $|im|$ stands for the positive dot product between two directions i and m.

The statistical distribution of the microfacet normals $D(m)$ is a strictly positive function of unit inverse steradian (sr^{-1}), such that $D(m)=0$ if $m \cdot n \leqslant 0$. The sum of the projected microfacet areas should be equal to the macroscopic surface, implying $\int_{\Omega_+(n)} D(m)(m.n)\ dm = 1$. Several distribution functions have been proposed in the literature, with the above properties. They are defined using one parameter [BS63, ON94, WMLT07], or more [LKYU12, BSH12, Bur12], to control the surface state.

The geometrical attenuation function $G(i,o,m)$ accounts for self-masking and self-shadowing effects. The widely used function from Torrance and Sparrow [TS67] makes the assumption that the micro-surface corresponds to a series of two dimensional V-cavity profile. This model is mathematically consistent but physically unrealistic [Hei14]. Nowadays, it is commonly admitted that

the Smith-Bourlier GAF [Smi67, BBS02] is closest to the physical behavior of micro-perturbed surfaces. Shadowing and masking are considered as independent, and the GAF $G(i,o,m)$ is thus approximated using the product of the same two functions G_1:

$$G(i,o,m) = G_1(i,m)\ G_1(o,m). \tag{2}$$

The most important assumption in the Smith-Bourlier GAF model is that micro-facets normals are not correlated, even in close proximity. Mathematically, this assumption can be written as follows:

$$G_1(v,m) \ = \ \begin{cases} G_1(v) & v\cdot m \geqslant 0 \\ 0 & v\cdot m < 0 \end{cases} \tag{3}$$

It has been used by Ashikhmin et al. [APS00] to derive the following expression:

$$G_1(v) = \frac{(v\cdot n)}{\int_{\Omega_+(v)}(v\cdot m')D(m')\ dm'}. \tag{4}$$

Other expressions of this function can be obtained, starting from the work of Bourlier [BBS02]. Walter et al. [WMLT07] and more recently Heitz [Hei14] express the normal distribution in the slopes space $P_{22}(p,q)$:

$$P_{22}(p,q) = \cos^4\theta_m\ D(m), \tag{5}$$

where p and q correspond to the surface slopes in the local coordinate system, defining the normal m, such that $p^2+q^2=\tan^2\theta_m$. The one dimensional distribution of slopes in the incidence plane is given by:

$$P_2(q) = \int_{-\infty}^{+\infty} P_{22}(p,q)\ dp. \tag{6}$$

Finally, $G_1(v)$ is obtained by the integration of P_2:

$$G_1(v) = \frac{1}{1+\Lambda(v)}, \tag{7}$$

where $\Lambda(v) = \frac{1}{\mu}\int_{-\infty}^{+\infty}(q-\mu)P_2(q)\ dq$ and $\mu = \cot\theta_v$. A formal proof of these derivations is given by Heitz in [Hei14].

Note that this GAF version is used by most rendering systems, though the discussion proposed by Ross et al. [RDP05] or Heitz et al. [HBP13] expresses correlated versions between masking and shadowing, considered as physically more plausible. In this paper, all the renderings are made with the uncorrelated version of the GAF only, and the additional material file provides the mathematical developments and some results with a correlated GAF.

For computer graphics, Beckmann's distribution [BS63] and GGX [TR75, WMLT07, Bur12] are the most popular functions. They can be derived analytically for the Smith-Bourlier GAF described above, and they are also interesting for importance sampling since the cumulative distribution function associated with $D(m)|mn|$ can be analytically expressed and inversed. GGX distribution exhibits a thinner bell shape with a longer tail than that of Beckmann. This latter property induces unusual BSDF behavior for GGX at grazing viewing angles but it is appreciated for other purposes such as fitting measured data. GGX introduced in computer graphics by Walter et al. [WMLT07] actually corresponds to the distribution proposed by Trowbridge and Reitz [TR75] and generalized by Burley [Bur12]. This latter distribution, denoted as GTR, uses an additional parameter γ which allows to control the tail of the normal distribution curve. This shape control feature is mandatory to represent more complex micro-surface distributions, as pointed out by Hoffman [Hof16].

$$D^{GTR}(m) = \frac{(\gamma-1)(\sigma^2-1)}{\pi(1-\sigma^{2-2\gamma})\ \cos^{2\gamma}\theta_m\ (\sigma^2+\tan^2\theta_m)^\gamma}. \tag{8}$$

When $\gamma=2$, the GTR distribution is exactly the GGX case. Unfortunately, to our knowledge, GTR distribution has no analytic masking function (except for the GGX case mentioned above). This paper fills this gap with a new formulation compatible with: (i) The analytic Smith-Bourlier masking function; (ii) Importance sampling. In addition, our distribution function naturally converges towards Beckmann's when $\gamma\to\infty$, contrary to GTR.

3. Student's t Normal Distribution

In addition to the GTR distribution, some authors have addressed this question of shape control [BSH12, BM14, HP15], but none of them provide an analytical derivation of the Smith's GAF. We aim at proposing a family of distributions associated with an analytical Smith's GAF and importance sampling functions. Our solution is inspired by GTR, with the following normalized general expression:

$$D^G(\theta_m) = \frac{(C-1)B}{\pi\cos^4\theta_m\left(1+B\tan^2\theta_m\right)^C}, \tag{9}$$

with $B\neq 0$ and $C\neq 1$. In the slopes space, this family corresponds to the standard bivariate Student's t-distribution:

$$P^G_{22}(p,q) = \frac{(C-1)B}{\pi\left(1+B(p^2+q^2)\right)^C}, \tag{10}$$

where B and C control the shape of the distribution. When $B=\frac{1}{\sigma^2}$ and $C=2$, D^G exactly corresponds to GGX, and when $C\to\infty$, the product BC tends to $\frac{1}{\sigma^2}$ and D^G tends to Beckmann's distribution. A detailed discussion and the mathematical analysis are provided in the additional file.

This representation also includes the Hyper-Cauchy definition (with $C=\gamma$ and $B=\frac{1}{\sigma^2}$), first introduced by Wellems et al. [WOB*06], and used by Butler and Marciniak [BM14] for fitting measured BRDFs. This latter includes GGX when $\gamma=2$ and becomes a dirac distribution when $\gamma\to\infty$; Beckmann's distribution does not appear. In practice, when γ increases, the surface becomes smoother, which already corresponds to the role of the roughness parameter σ. This reduces the interest of this additional parameter γ for the shape control of the distribution.

Instead, we propose to use $B=\frac{1}{\sigma^2(\gamma-1)}$, and the resulting new sub-family of distribution of normals is denoted as STD in this paper (standing for *Student's T-Distribution*):

$$D^{STD}(m) = \frac{(\gamma-1)^\gamma\sigma^{2\gamma-2}}{\pi\cos^4\theta_m\left((\gamma-1)\sigma^2+\tan^2\theta_m\right)^\gamma}, \tag{11}$$

where $\gamma>1$ controls the shape of the distribution bell. Statistically speaking, γ represents the number of samples modeled by a bivariate Student's t-distribution. When $\gamma=2$, STD remains equal to GGX

and when $\gamma \to \infty$, STD still tends to Beckmann's distribution (using a Taylor series, as shown in the supplemental material), contrary to Hyper-Cauchy. The additional material file contains further discussions concerning the general distribution (Equations 9 and 10), as well as the derivations for the corresponding Smith's GAF.

In practice, we use γ=40 for a close approximation of Beckmann's distribution (see Section 5). Figure 1 illustrates some examples of the visual appearance variations according to γ. Figure 3 shows the general shape of the slopes distribution and the GAF, for several values of γ and σ.

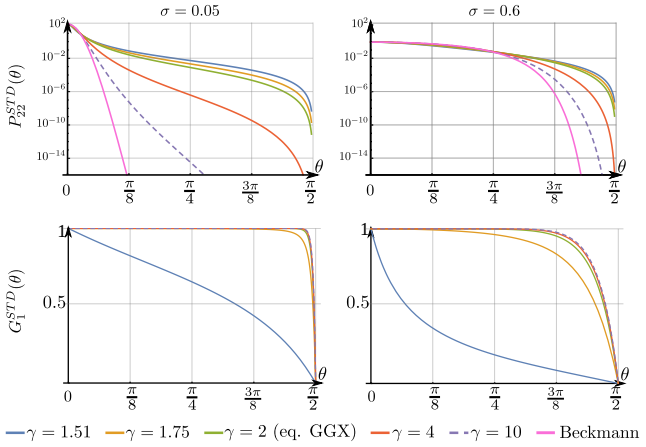

Figure 3: *Distribution of slopes P_{22} for STD (first row, in log scale) and corresponding G_1 function (second row), for different values of γ and σ. Each curve corresponds to a value of γ: When γ=2, STD corresponds mathematically to GGX.*

3.1. Shadowing and masking

The analytic Smith-Bourlier GAF associated to our distribution is derived according to the mathematical process detailed by Heitz in [Hei14] and summarized in Section 2. Equation 11 is expressed in the slopes space:

$$P_{22}^{STD}(m) = \frac{(\gamma\text{-}1)^{\gamma}\sigma^{2\gamma-2}}{\pi\left((\gamma\text{-}1)\sigma^2+\tan^2\theta_m\right)^{\gamma}}, \tag{12}$$

$\Lambda(v)$ is defined as:

$$\Lambda(v) = \frac{\Gamma(\gamma\text{-}\frac{1}{2})}{\Gamma(\gamma)\sqrt{\pi}}\left(\frac{(\gamma\text{-}1)^{\gamma}}{2\gamma\text{-}3}S_1^{\gamma}(\mu)+\sqrt{\gamma\text{-}1}S_2^{\gamma}(\mu)\right)\text{-}\frac{1}{2}, \tag{13}$$

where $\mu=\cot\theta_v$, and

$$S_1^{\gamma}(\mu) = \frac{\sigma\left((\gamma\text{-}1)+\frac{\mu^2}{\sigma^2}\right)^{\frac{3}{2}\text{-}\gamma}}{\mu}, \tag{14}$$

$$S_2^{\gamma}(\mu) = \frac{\mu}{\sigma}\times{}_2F_1\left(\frac{1}{2},\gamma\text{-}\frac{1}{2};\frac{3}{2};\frac{\text{-}\mu^2}{(\gamma\text{-}1)\sigma^2}\right), \tag{15}$$

with $\Gamma(x)$, the Eulerian gamma function and ${}_2F_1$, the Gauss hypergeometric function. Finally, the GAF function G_1^{STD} is written using Equation 7. Figure 3 illustrates the curves corresponding to P_{22}^{STD} (first row) and G_1^{STD} with several values of γ and σ. G_1^{STD} varies more widely for $1.5<\gamma<4$ which highly impacts the visual appearance, while the change is smoother otherwise.

Note that STD should be used in practice only with $\gamma\in]1.5,\infty)$, since G_1^{STD} is undefined for $\gamma<1.5$. When $\gamma\to 1.5$, STD tends to the Cauchy distribution and the GAF value tends to 0. In this case, the material would correspond to microfacets either aligned with or perpendicular to the surface, their area is infinite for γ=1.5 (which is physically not plausible) and light multiple reflections would be predominant. As previously mentioned, when γ=∞, STD is actually a Gaussian distribution in slopes space corresponding to that of Beckmann's normal distribution.

3.2. Isotropic Importance sampling

Importance sampling should also be provided with any BRDF model used in computer graphics. The cumulative density fonction (cdf) associated with $p(m)=D^{STD}(m)|mn|$ can be defined and inverted analytically. The resulting formulation is:

$$\varphi = 2\pi\xi_1, \tag{16}$$

$$\theta = \arctan\left(\sigma\sqrt{(\gamma-1)\left((1\text{-}\xi_2)^{\frac{1}{1-\gamma}}\text{-}1\right)}\right), \tag{17}$$

with (ξ_1,ξ_2) two uniform random numbers in $[0,1)^2$.

3.3. Anisotropy

Our STD distribution function is *shape invariant* † [Hei14, Hof16] thus easily derivable for anisotropic materials:

$$D_{aniso}^{STD}(m) = \frac{1}{\pi\sigma_x\sigma_y\cos^4\theta_m\left(1+\frac{\tan^2\theta_m}{\gamma\text{-}1}\left(\frac{\cos^2\varphi_m}{\sigma_x^2}+\frac{\sin^2\varphi_m}{\sigma_y^2}\right)\right)^{\gamma}}, \tag{18}$$

where σ_x and σ_y correspond to the roughnesses associated with the surface local coordinate system. The mathematical derivations for the geometric attenuation function are the same as those of the isotropic case, the $\Lambda(v)$ function is obtained thanks to Equations 14 and 15 using:

$$\frac{\sigma}{\mu} = \tan\theta_v\sqrt{\sigma_x^2\cos^2\varphi_v+\sigma_y^2\sin^2\varphi_v}.$$

In the anisotropic case, the cdf can also be defined and inverted analytically, leading to:

$$\varphi = \arctan\left(\frac{\sigma_y}{\sigma_x}\tan(2\pi\xi_1)\right), \tag{19}$$

$$\theta = \arctan\sqrt{\frac{(1\text{-}\xi_2)^{\frac{1}{1-\gamma}}\text{-}1}{A}}, \tag{20}$$

with

$$A = \frac{\left(\frac{\cos^2\varphi}{\sigma_x^2}+\frac{\sin^2\varphi}{\sigma_y^2}\right)}{\gamma\text{-}1},$$

and (ξ_1,ξ_2) two uniform random numbers in $[0,1)^2$.

† i.e. it can be represented in the form $f(\frac{\tan\theta}{\sigma})/(\sigma^2\cos^4\theta)$

4. Specific functions and GAF approximation

The analytical Smith-Bourlier GAF associated with STD makes use of Γ and ${}_2F_1$ functions, as shown in Equations 13 and 15. These functions are complex to evaluate and increase the computation time. This is why we propose some simple alternatives with discrete values of gamma and an approximate solution.

4.1. Functions using discrete values of γ

Γ and ${}_2F_1$ can be replaced without approximation by finite sums. These latter finally simplify, and the Λ function becomes:

$$\Lambda(v)=(\gamma\text{-}1)A_1\left(\frac{\sigma}{\mu}\sqrt{\gamma\text{-}1}\frac{(1+\frac{\mu^2}{(\gamma\text{-}1)\sigma^2})^{3/2-\gamma}}{2\gamma\text{-}3}\text{-}A_2\right), \tag{21}$$

where two cases can be distinguished for integer and half integer values of γ (i.e. $\gamma\in\{\mathbb{N}\mid\gamma>1\}$ and $\gamma\in\{n+1/2\mid n\in\mathbb{N}\ \&\ n\geq 2\}$ respectively), for A_1 and A_2.

Integer values of γ:

$$A_1=\frac{(2\gamma\text{-}2)!}{4^{\gamma\text{-}1}(\gamma\text{-}1)!^2},$$

and

$$A_2 = \sum_{k=0}^{\gamma-2}\binom{\gamma\text{-}2}{k}\frac{(\text{-}1)^k}{2k+1}A_3(k),$$

$$A_3(k) = 1\text{-}\left(\frac{\mu}{\sigma\sqrt{(\gamma\text{-}1)+\frac{\mu^2}{\sigma^2}}}\right)^{2k+1}.$$

Half integer values of γ:

$$A_1=\frac{2}{\pi}\sum_{k=0}^{\gamma-3/2}\binom{\gamma-3/2}{k}\frac{(-1)^k}{2k+1},$$

and

$$A_2=\frac{1}{2^{2\gamma-4}}A_{21}+\frac{1}{2^{2\gamma-3}}A_{22},$$

where:

$$A_{21} = \sum_{k=0}^{\gamma-5/2}\binom{2\gamma-3}{k}\frac{1}{2\gamma-3-2k}\times \left(-\sin\left((2\gamma-3-2k)\arctan\left(\frac{\mu}{\sqrt{(\gamma-1)\sigma}}\right)\right)\right)$$

$$A_{22} = \binom{2\gamma-3}{\gamma-3/2}\left(\frac{\pi}{2}-\arctan\left(\frac{\mu}{\sqrt{(\gamma-1)\sigma}}\right)\right)$$

4.2. GAF approximation

The general model can also be approximated closely using the following rational fractions instead of Equation 15:

$$S_2^{\gamma}(z)\approx F_{21}(z)\left(F_{22}(\gamma)+F_{23}(\gamma)\cdot F_{24}(z)\right), \tag{22}$$

where $z=\mu/\sigma$ and

$$\begin{aligned}
F_{21}(z) &= \frac{1.066z+2.655z^2+4.892z^3}{1.038+2.969z+4.305z^2+4.418z^3},\\
F_{22}(\gamma) &= \frac{14.402\text{-}27.145\gamma+20.574\gamma^2\text{-}2.745\gamma^3}{\text{-}30.612+86.567\gamma\text{-}84.341\gamma^2+29.938\gamma^3},\\
F_{23}(\gamma) &= \frac{\text{-}129.404+324.987\gamma\text{-}299.305\gamma^2+93.268\gamma^3}{\text{-}92.609+256.006\gamma\text{-}245.663\gamma^2+86.064\gamma^3},\\
F_{24}(z) &= \frac{6.537+6.074z\text{-}0.623z^2+5.223z^3}{6.538+6.103z\text{-}3.218z^2+6.347z^3}.
\end{aligned} \tag{23}$$

Figure 4 illustrates the computation time differences for our expressions of STD (real, integer, half integer and approximate) and two configurations corresponding to Beckmann's (exact and rational approximation [WMLT07]) distributions. The first row shows the computation time obtained using random evaluations of the distribution, the GAF and importance sampling; this process only accounts for the computation time corresponding to the BSDF evaluation. The second row corresponds to the computation time observed for a practical rendering configuration of a rough gold material, including ray-scene intersection, path tracing multiple reflections, light sources sampling, etc. The curves illustrate the efficiency of both the integer exact configuration and the approximate GAF representation, with computation time slightly higher than those obtained with Beckmann's distributions. However, contrary to our expectations, the half-integer version can even be slower than the exact formulation when γ or σ increase.

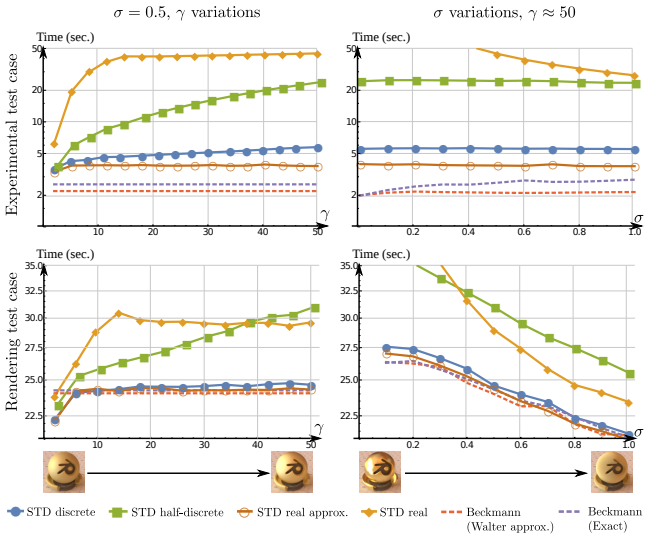

Figure 4: *Distribution, GAF and sampling computation time with variations of γ and σ, (first row) corresponding only to the BSDF evaluation, and (second row) in a practical rendering test case including Monte Carlo path tracing, with a rough gold object.*

The relative error corresponding to the approximate model compared to the exact formulation is illustrated in Figure 5, where the GAF difference is integrated over the hemisphere. In the worst case,

the cumulated error is less than 0.7%. Figure 6 illustrates the error distribution for a given scene, according to σ and γ. The differences are very low and difficult to distinguish for an observer. The difference images corresponding to the right column essentially exhibit noise due to Monte Carlo variance. We believe that the approximation of STD we propose corresponds to a good compromise in terms of both visual quality and performances.

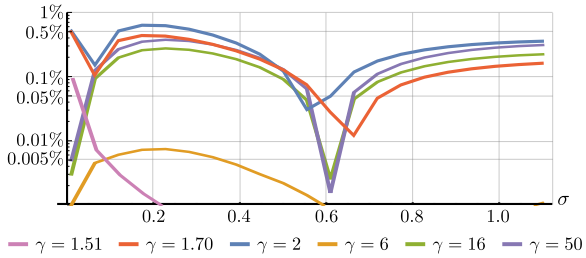

Figure 5: *Relative error of our approximate G_1 function according to σ, integrated over the hemisphere and given in percentage. The maximum error value is below 0.7%.*

5. Results

STD and its associated Smith-Bourlier GAF have been implemented in the Mitsuba renderer [Jak10]. Special functions Γ and ${}_2F_1$ appearing in Equations 13 and 15 come from the *GNU Scientific Library* [Gou09]. The results presented below have been produced with an intel Core i7-3740QM, 2.7 GHz CPU.

Figure 7 illustrates the panel of materials corresponding to a rough aluminium surface (modeled by the *rough conductor* material implemented in Mitsuba). The most visible changes correspond to $\gamma \in]3/2;4]$, for a set of roughness values σ. When $\gamma \to 1.5$, the surface becomes darker, due to the GAF function. As explained in Section 3.1, in this case the surface is covered with many almost vertical microfacets. When increasing σ while decreasing γ, a part of the light energy is not taken into account (no multiple reflections). Figure 9 illustrates the percentage of reflected energy when ignoring multiple scattering between microfacets. This percentage is estimated according to an energy balance test which should be equal to 1 when the whole energy is reflected by the surface:

$$\int_{\Omega_+(i)} \int_{\Omega_+(o)} f(i,o,n)|in||on|do\,di = 1, \tag{24}$$

where $f(i,o,n) = \frac{F(i,h)D(h)G(i,o,h)}{4|ih||oh|}$ is the BSDF of a rough specular material, with h the half angle vector between i and o and the Fresnel term $F = 1$, which corresponds to perfectly reflective microfacets. Equation 24 is generally not verified in practice when single scattering alone is used; GGX distribution suffers from this more than Beckmann's distribution due to its higher tail. In any case, for low values of γ and high values of σ, light multiple scattering between microfacets should be handled but few previous work deals with this issue. The method proposed by Heitz et al. [HHdD16] is the latest and can also be applied with STD but this approach is based on the importance sampling from visible microfacets normals proposed by Heitz and d'Eon [HD14]. This latter is more difficult to provide analytically, since the STD cumulative distribution

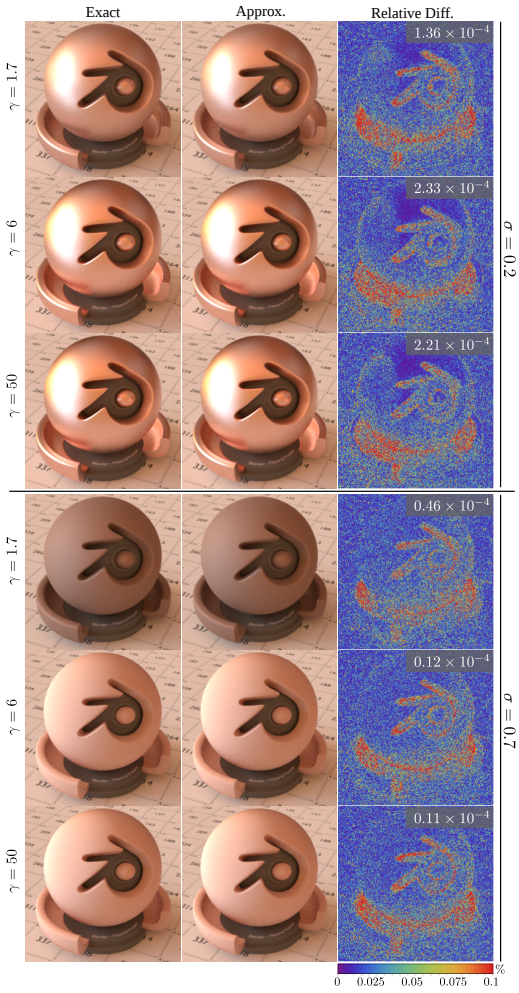

Figure 6: *Visual comparison between exact and approximate model with a rough copper material. False color images represent the relative difference between both renderings and the RMSE is given in the top right corner of each image.*

function cannot be analytically inversed. The authors recommend to precompute a set of values for this function according to σ, and store them in a table. However, for STD an additional 2D table is required to deal with the values of γ. This question is discussed in the supplemental material file, which also contains a procedure for pseudo-visible normals sampling for a more practical use of STD.

Figures 1 and 8 illustrate the use of STD with several opaque or transparent materials (rough gold, rough copper, rough plastic, rough diamond and rough anisotropic aluminium). Note that the loss of energy due to multiple scattering is partially masked in rough plastic material by the diffuse reflection component.

Mathematically, STD tends to Beckmann when $\gamma \to \infty$ (Figure 3). In practice a good approximation of this distribution can be obtained for $\gamma \geqslant 30$ (see Figure 10). The visual difference is not visible and the error for γ=40 is below 1% when $\sigma < 1.2$.

STD covers an infinite set of microfacets configurations from

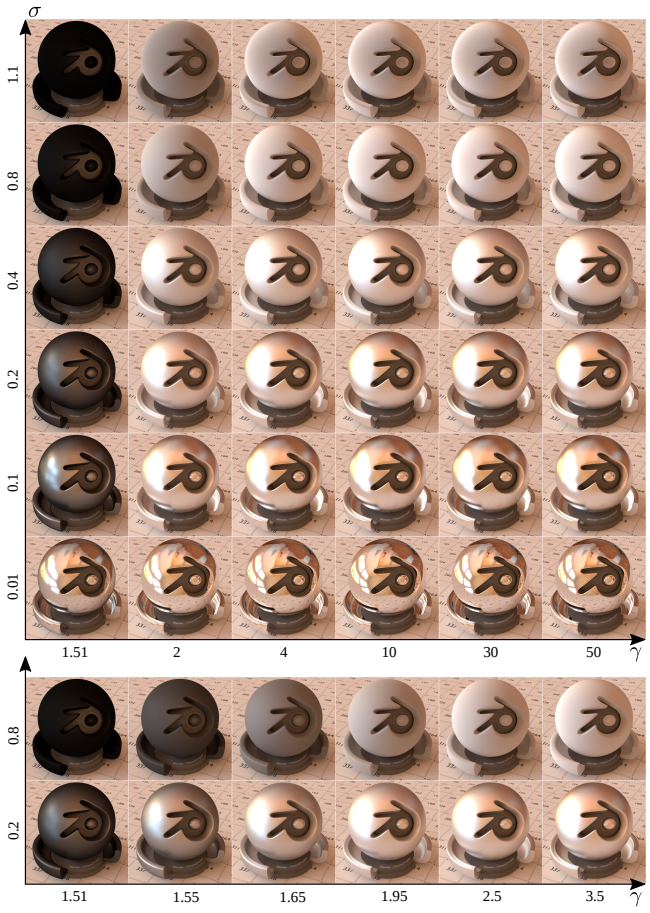

Figure 7: *The visual impact of the STD distribution and its GAF when the tail parameter* γ *and the roughness parameter* σ *change for a rough conductor material.*

$\gamma > 1.5$ to Beckmann ($\gamma \to \infty$) and equal to GGX when γ=2. This feature is interesting for fitting measured materials since the distribution bell can be adapted. We have fitted the complete MERL database [MPBM03], using a genetic algorithm based on the normalized absolute distance between data and the model to fit. The fitting method is described more precisely in the supplemental material. Figure 11 provides a comparison of the final measured error resulting from the fitting of all MERL data, using several microfacet distributions: Beckmann [BS63], GGX [WMLT07], Löw [LKYU12], and STD. The complete BRDF model used corresponds to Cook-Torrance [CT82] representation: A Lambertian term associated with a distribution of specular microfacets. As expected, STD distribution always provides lower errors compared with that of Beckmann and GGX. Besides, Löw's BRDF provides a lower error for some glossy materials, but STD remains better in most cases. Löw's model corresponds to a different representation, which uses Torrance-Sparrow GAF [TS67] (the Smith GAF cannot be derived analytically), with another class of distributions, especially designed for fitting MERL materials. Note that the fitting process highly depends on the chosen error function, and we believe that the process of fitting measured data still remains an open problem, which depends on the target application. For instance, a lower error during the fitting process does not always ensure visually better images (as illustrated for several data in the supplemental material).

6. Conclusion and future work

Microfacet based BSDFs are widely used in the computer graphics community since they are physically plausible, controlled by only few parameters, and intuitive to manage. They are built upon a statistical distribution of small facets, which should be carefully chosen, so as to manage the associated geometric attenuation factor and importance sampling schemes. These constraints are met with only few distributions, namely Beckmann's and GGX.

This paper presents a new more generalized distributions family of microfacets normals, based on the bivariate Student's t-distribution in slopes space. It particularly details one sub-family, denoted as STD, which meets the above constraints and offers an infinite set of configurations including both Beckmann's and GGX: We provide the analytical geometric attenuation factor from Smith and importance sampling.

In addition, for performance considerations, we propose practical formulations of STD with discrete values of γ and an approximate version. This latter can be used for interactive rendering systems without noticeable loss of quality.

As mentioned above, multiple scattering in microfacets remains challenging to handle and strongly impact the visual aspect of a material. We wish to investigate this issue and propose if possible an analytical solution with STD according to the approach proposed in [HHdD16]. We would also like to propose a formulation of the importance sampling for STD, based on the visible normals [HD14].

References

[APS00] ASHIKMIN M., PREMOŽE S., SHIRLEY P.: A microfacet-based brdf generator. In *ACM SIGGRAPH proceedings* (2000). 2, 3

[BBS02] BOURLIER C., BERGINC G., SAILLARD J.: One- and two-dimensional shadowing functions for any height and slope stationary uncorrelated surface in the monostatic and bistatic configurations. *IEEE Transactions on Antennas and Propagation 50*, 3 (2002). 2, 3

[BM14] BUTLER S. D., MARCINIAK M. A.: Robust categorization of microfacet brdf models to enable flexible application-specific brdf adaptation. In *SPIE 9205, Reflection, Scattering, and Diffraction from Surfaces IV* (September 2014). 3

[BS63] BECKMANN P., SPIZZICHINO A.: *The scattering of electromagnetic waves from rough surfaces*. Pergamon Press, 1963. 2, 3, 7

[BSH12] BAGHER M. M., SOLER C., HOLZSCHUCH N.: Accurate fitting of measured reflectances using a shifted gamma micro-facet distribution. *Computer Graphics Forum 31*, 4 (June 2012). 2, 3

[Bur12] BURLEY B.: Physically-based shading at disney. In *ACM SIGGRAPH 2012 Courses* (2012). 2, 3

[CT82] COOK R. L., TORRANCE K. E.: A reflectance model for computer graphics. In *ACM SIGGRAPH proceedings* (1982). 2, 7

[CTL89] CHURCH E., TAKACS P., LEONARD T.: The prediction of brdfs from surface profile measurements. In *SPIE 1165* (1989). 2

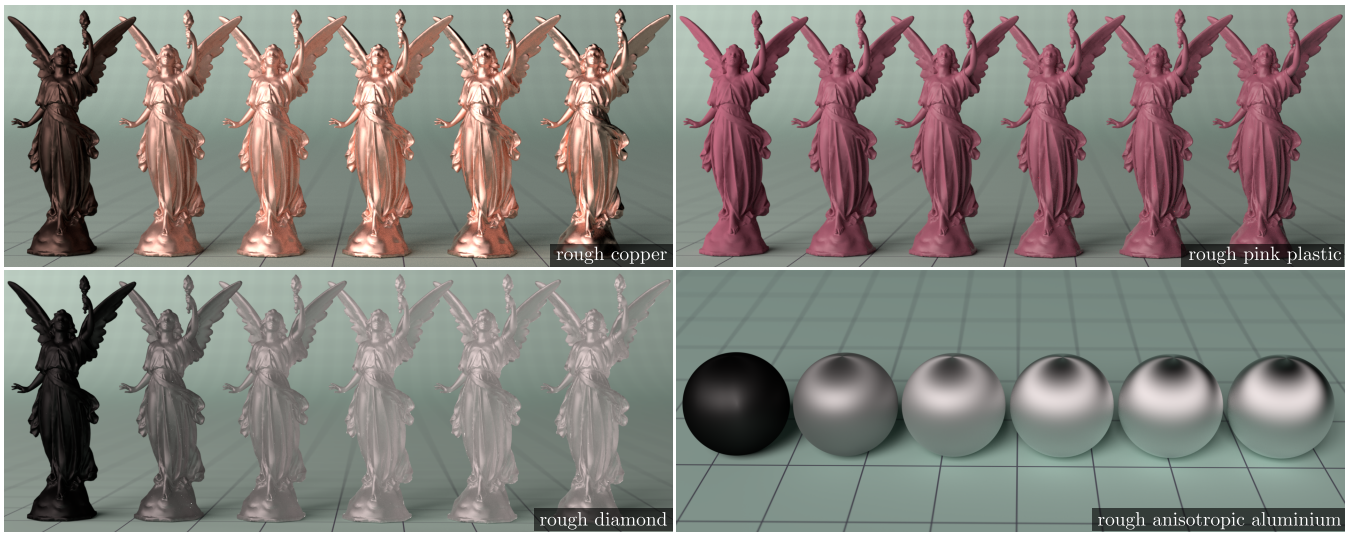

Figure 8: *Various glossy materials rendered with STD: (top left) Rough metallic, gold; (top right) Rough plastic, with a Lambertian chroma; (bottom left) Rough dielectric transparent diamond; (bottom right) Anisotropic rough metallic, aluminium. Isotropic materials are defined using* $\sigma = 0.3$ *and several values for* γ *from left to right:* $\gamma = [1.51, 1.65, 2, 4, 10, 50]$*, while anisotropic materials are defined using* $\sigma_x = 0.7$ *and* $\sigma_y = 0.3$*, for the same values of* γ*.*

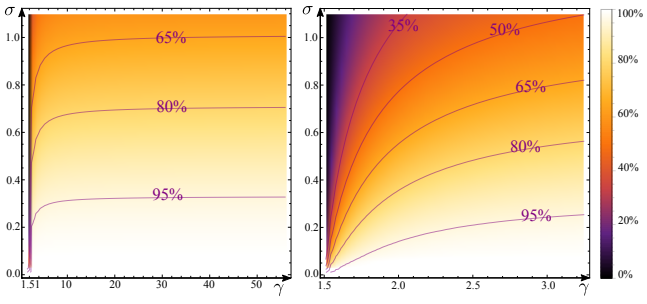

Figure 9: *Energy conservation percentage for perfect mirror microfacets, with single scattering: The unreflected light corresponds to ignored light multiple reflections. For low values of* γ*, the distribution tends to produce higher tails, resulting in darker materials with consequently lower energy conservation values.*

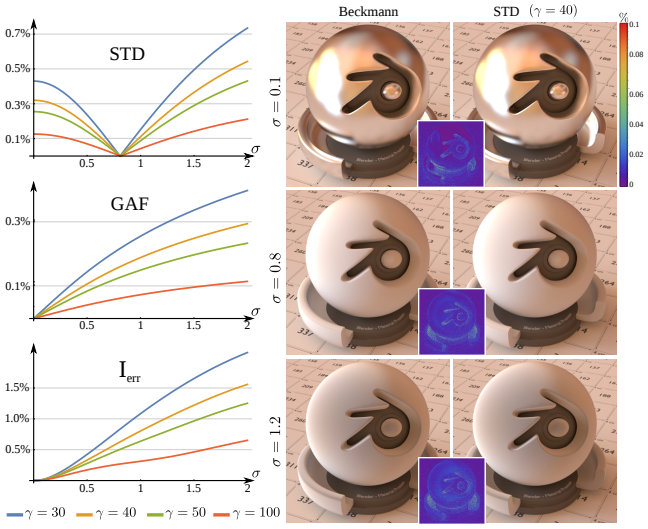

Figure 10: *Relative error between our STD distribution and Beckmann depending on* σ*, for* $\gamma = \{30, 40, 50, 100\}$*. When* $\sigma < 1.2$*, the approximation of Beckmann by STD with* $\gamma = 40$ *ensures an error below* 0.5% *for the distribution and below* 0.3% *for the GAF.* I_{err} *provides the relative error for the energy balance test (Equation 24), according to* σ*. False color coded images represent the relative error in percentage.*

[DHI*13] DUPUY J., HEITZ E., IEHL J.-C., POULIN P., NEYRET F., OSTROMOUKHOV V.: Linear efficient antialiased displacement and reflectance mapping. *ACM Transactions On Graphics, SIGGRAPH Asia proceedings 32*, 6 (2013). 2

[Gou09] GOUGH B.: *GNU Scientific Library Reference Manual - Third Edition*, 3rd ed. Network Theory Ltd., 2009. URL: http://www.gnu.org/software/gsl/. 6

[HBP13] HEITZ E., BOURLIER C., PINEL N.: Correlation effect between transmitter and receiver azimuthal directions on the illumination function from a random rough surface. *Waves in Random and Complex Media 23*, 3 (Aug. 2013). 3

[HD14] HEITZ E., D'EON E.: Importance sampling microfacet-based bsdfs using the distribution of visible normals. *Computer Graphics Forum, EGSR proceedings 33*, 4 (July 2014). 6, 7

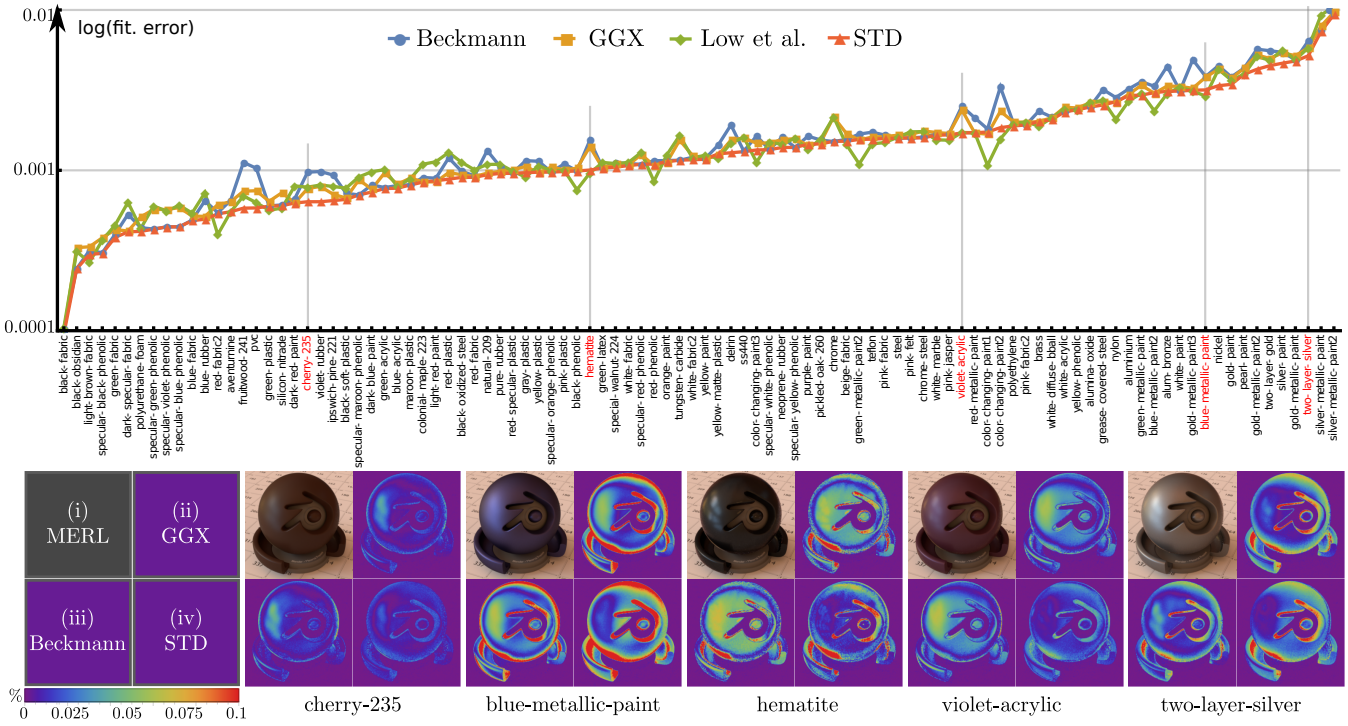

Figure 11: *Normalized absolute difference (fit. error) for MERL database fitting, using specular dielectric microfacets (real refractive index and a constant Lambertian term). Comparisons (relative differences) between: (i) Measured data; (ii) Fitted GGX; (iii) Fitted Beckmann; and (iv) Fitted STD.*

[Hei14] HEITZ E.: Understanding the masking-shadowing function in microfacet-based brdfs. *Journal of Computer Graphics Techniques 3*, 2 (June 2014). 2, 3, 4

[HHdD16] HEITZ E., HANIKA J., D'EON E., DACHSBACHER C.: Multiple-scattering microfacet bsdfs with the smith model. *ACM Transactions On Graphics, SIGGRAPH Asia proceedings 35*, 4 (August 2016). 6, 7

[Hof16] HOFFMAN N.: Recent advances in physically based shading. In *ACM SIGGRAPH 2016 Courses* (2016). 3, 4

[HP15] HOLZSCHUCH N., PACANOWSKI R.: *A physically accurate reflectance model combining reflection and diffraction*. Research Report RR-8807, INRIA, Nov. 2015. 3

[Jak10] JAKOB W.: Mitsuba renderer, 2010. URL: `http://www.mitsuba-renderer.org`. 6

[JdJM14] JAKOB W., D'EON E., JAKOB O., MARSCHNER S.: A comprehensive framework for rendering layered materials. *ACM Transactions on Graphics, SIGGRAPH proceedings 33*, 4 (July 2014). 2

[LKYU12] LÖW J., KRONANDER J., YNNERMAN A., UNGER J.: Brdf models for accurate and efficient rendering of glossy surfaces. *ACM Transactions On Graphics 31*, 9 (2012). 2, 7

[MPBM03] MATUSIK W., PFISTER H., BRAND M., MCMILLAN L.: A data-driven reflectance model. *ACM Transactions On Graphics, SIGGRAPH proceedings 22*, 3 (July 2003), 759–769. 7

[ON94] OREN M., NAYAR S. K.: Generalization of lambert's reflectance model. In *ACM SIGGRAPH proceedings* (1994). 2

[RDP05] ROSS V., DION D., POTVIN G.: Detailed analytical approach to the gaussian surface bidirectional reflectance distribution function specular component applied to the sea surface. *J. Opt. Soc. Am. A 22*, 11 (Nov 2005). 3

[Sch94] SCHLICK C.: An inexpensive brdf model for physically-based rendering. *Computer Graphics Forum 13*, 3 (1994). 2

[Smi67] SMITH B.: Geometrical shadowing of a random rough surface. *IEEE Transactions on Antennas and Propagation 15*, 5 (September 1967). 2, 3

[Sto67] STOGRYN A.: Electromagnetic scattering from rough, finitely conducting surfaces. *Radio Science 2*, 4 (1967). 2

[TR75] TROWBRIDGE T. S., REITZ K. P.: Average irregularity representation of a rough surface for ray reflection. *Journal of Optical Society of America 65*, 5 (May 1975). 2, 3

[TS67] TORRANCE K. E., SPARROW E. M.: Theory for off-specular reflection from roughened surfaces. *Journal of Optical Society of America 57*, 9 (Sep 1967). 2, 7

[WMLT07] WALTER B., MARSCHNER S. R., LI H., TORRANCE K. E.: Microfacet models for refraction through rough surfaces. In *Computer Graphics Forum, EGSR proceedings* (2007). 2, 3, 5, 7

[WOB*06] WELLEMS D., ORTEGA S., BOWERS D., BOGER J., FETROW M.: Long wave infrared polarimetric model: theory, measurements and parameters. *Journal of Optics A: Pure and Applied Optics 8*, 10 (2006). 3